

Supplementary material

Evaluation of climate variability and change in ACCESS historical simulations for CMIP6

Harun A. Rashid^{A,C}, Arnold Sullivan^A, Martin Dix^A, Daohua Bi^A, Chloe Mackallah^A, Tilo Ziehn^A,
Peter Dobrohotoff^A, Siobhan O'Farrell^A, Ian N. Harman^B, Roger Bodman^A and Simon Marsland^A

^ACSIRO Oceans and Atmosphere, 107–121 Station Street, Aspendale, Vic. 3195, Australia.

^BCSIRO Oceans and Atmosphere, Canberra, Australia.

^CCorresponding author. Email: harun.rashid@csiro.au

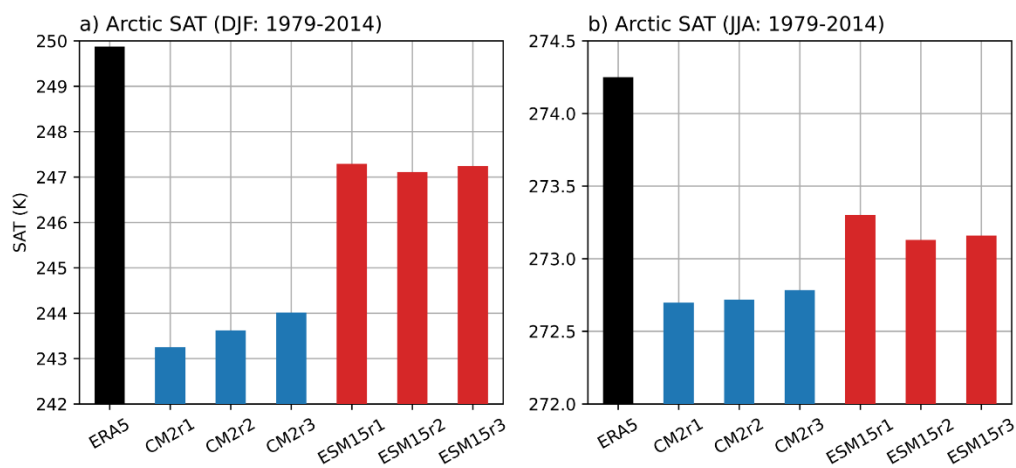


Figure S1. Seasonal mean surface-air temperatures averaged over the Arctic region (north of 70°N) for reanalysis (black bars), three-member ACCESS-CM2 (blue bars) and ACCESS-ESM1-5 (red bars) simulations. The means are calculated over the 1979-2014 period, to match the reanalysis, for a) DJF and b) JJA seasons. Note the difference in y-axis scales of a) and b).

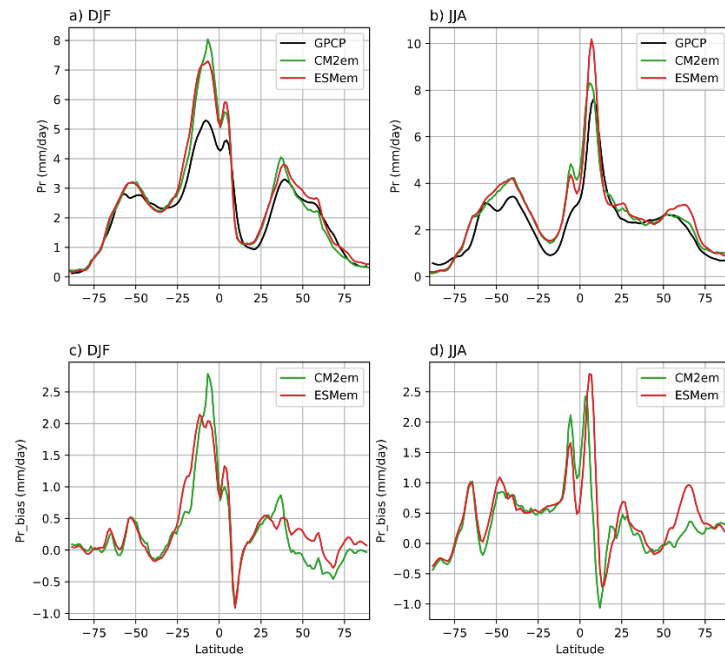


Figure S2. Latitudinal profiles of observed and simulated rainfall rates (mm day^{-1}). The upper panels show the absolute rainfall and the lower panels show the rainfall biases with respect to GPCP observations.

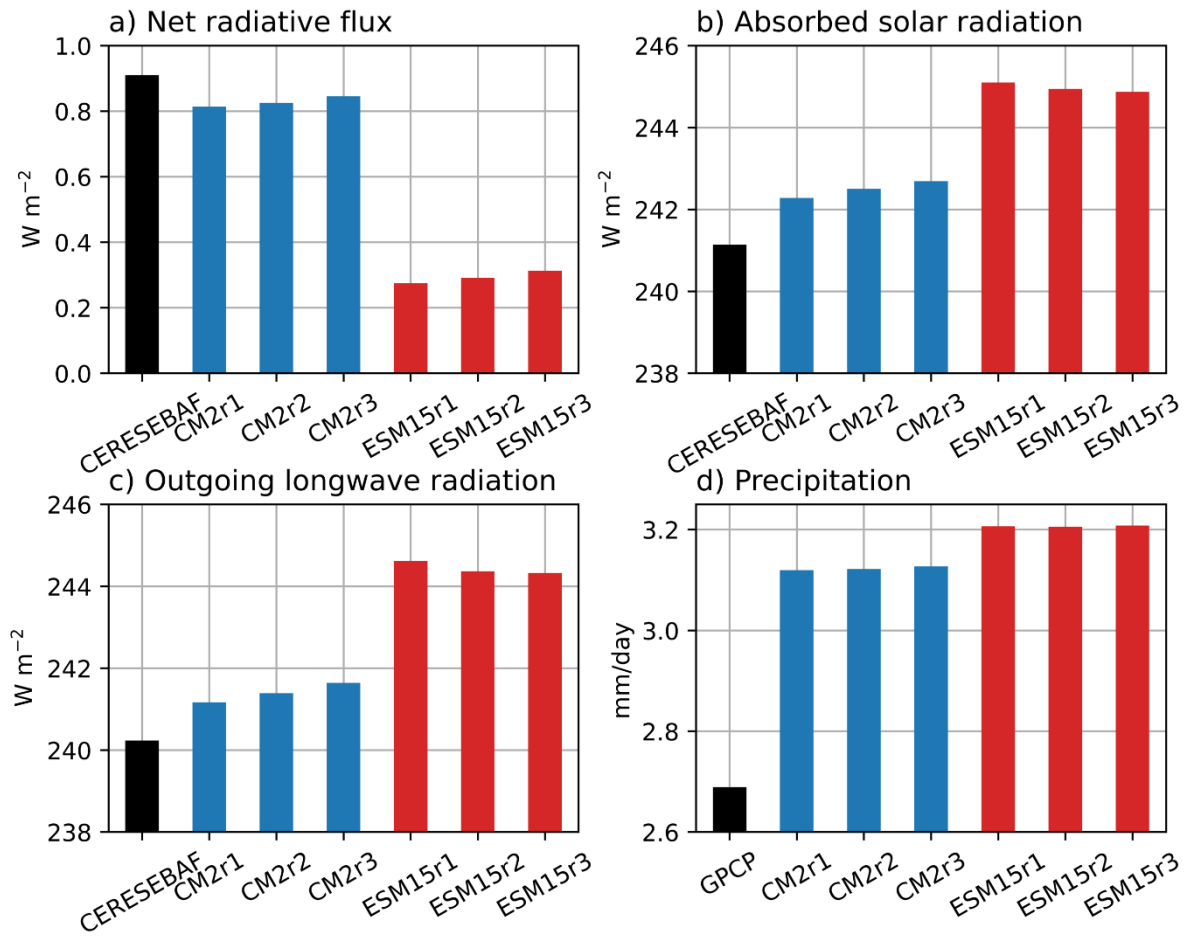


Figure S3. Global- and time-mean values of the a) net radiative flux at the top-of-the-atmosphere, b) absorbed shortwave radiation flux, c) outgoing longwave radiation flux, and d) precipitation rate. The radiative fluxes in a) and b) are positive downward.

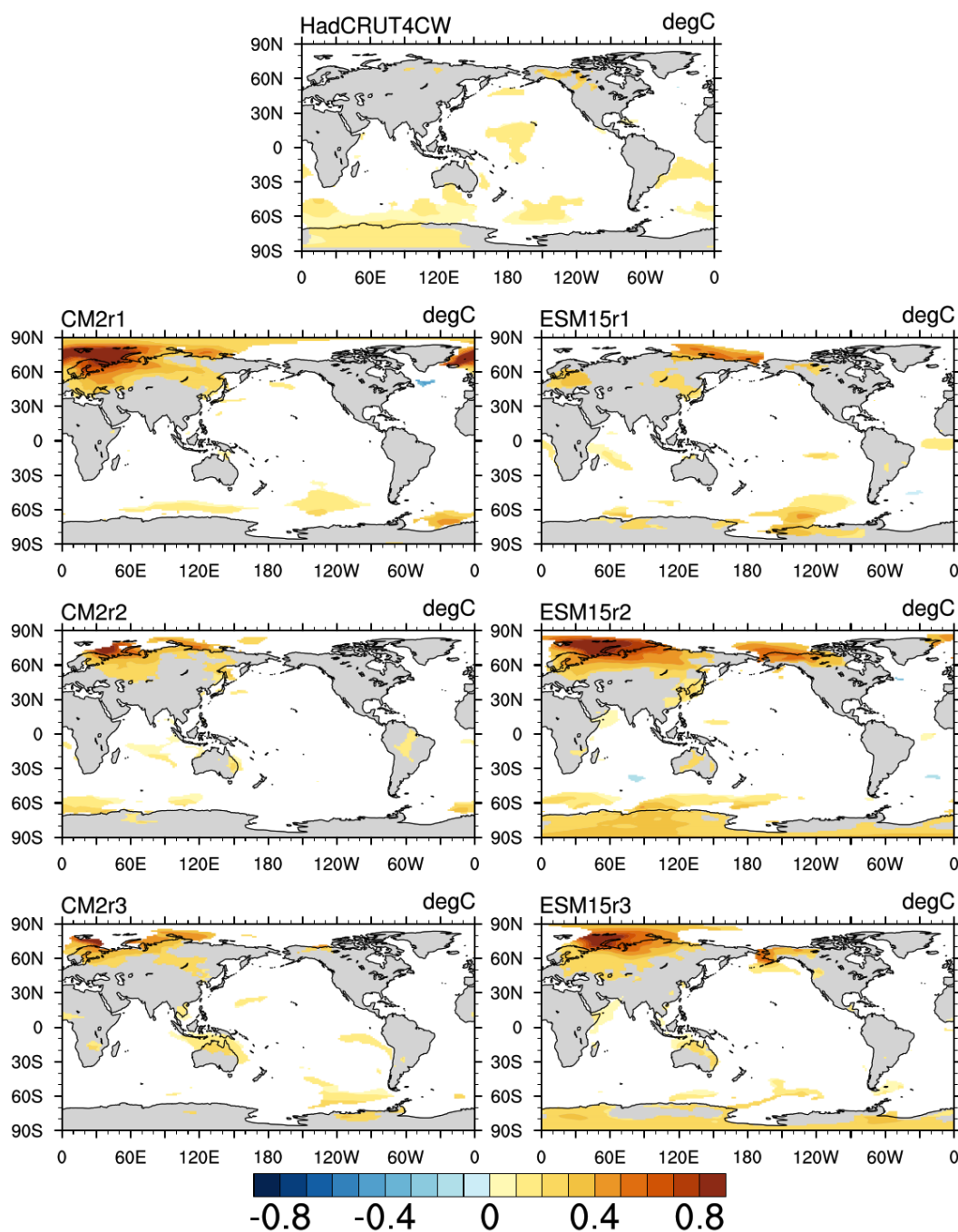


Figure S4. Spatial patterns of surface-air temperatures associated with the observed and simulated GMST residual timeseries. Shown are the regression coefficients of the surface-air temperature anomalies onto the corresponding standardised residual timeseries and, hence, the regression coefficients have the unit of degrees Celsius.